Ocean and Coastal Research

CASE REPORT

http://doi.org/10.1590/2675-2824072.23154
ISSN 2675-2824

Indonesia Cable-Based Tsunameter (InaCBT): Tsunami detection and identification on other seismic wave signals

Wahyu W. Pandoe[1]*, Michael A. Purwoadi[2], Zulfa Qonita[3], Alfi Rusdiansyah[3], Aris Suwarjono[4]

[1] Research Center for Hydrodynamic Technology – National Research and Innovation Agency (Technology-2 Building #251 – BJ Habibie Science and Technology Park PUSPIPTEK – Muncul – South Tangerang – BANTEN 15314 – Indonesia).
[2] Research Center for Electronics – National Research and Innovation Agency (Technology-3 Building #254 – BJ Habibie Science and Technology Park PUSPIPTEK – Muncul – South Tangerang – BANTEN 15314 – Indonesia).
[3] Research Center for Geological Disaster – National Research and Innovation Agency (JL. Sangkuriang – Kompleks BRIN – Coblong – Kota Bandung – Jawa Barat 40135 – Indonesia).
[4] Research Center for Artificial Intelligence and Cyber Security – National Research and Innovation Agency (Technology-3 Building #254 – BJ Habibie Science and Technology Park PUSPIPTEK – Muncul – South Tangerang – BANTEN 15314 – Indonesia)

* Corresponding author: wahy009@brin.go.id

ABSTRACT

The Indonesian Cable-Based Tsunameter (InaCBT) is the most recently developed innovative prototype that has been deployed in the Flores Sea north of Labuan Bajo, Flores Island, Indonesia. Two ocean bottom units (OBU) were attached to a single fiber-optic cable. The first one is 34.0 km from the shore at a depth of 2100 m (LB-01) and the second one is 54.2 km from the shore at depth of 4110 m (LB-02), respectively. Each OBU comprises one deep-sea bottom pressure recorder (BPR); a three-axis accelerometer; and temperature, humidity, and leakage sensors. Since deployment, the InaCBT has detected at least three near-field and distant earthquake events. One of them, the M7.5 Banda earthquake (EQ), detected on January 9, 2023, resulted a rise of the sea level recorded at six coastal tidal stations around the location. Near real-time analysis applies Lanczos filtering to split EQ signals (high frequency) and tsunamis (low frequency, if present). EQ wave signals dominate at 10-14-second wave periods. Using data from Banda EQ, the low-frequency wave shows an oscillation that probably indicates the presence of a tsunami wave. The identification and distinction of EQs and tsunami can be done by directly filtering raw data without detiding and by using harmonic analysis. The 30-50-second cut-off period can separate EQ and tsunami signals.

Keywords: Tsunami early warning, Deep sea pressure, Lanczos filtering, Seismic and tsunami signals, Spectral analysis

INTRODUCTION

The Indonesian Government established the Indonesian Tsunami Early Warning System (InaTEWS) in 2005, responding to the devastating tsunami of Aceh in December 2004. The system became officially operational as a national Program in November 2008, aiming to observe and report earthquakes (EQs) and tsunamis. This national program covers an end-to-end structure to sense EQs and tsunamis and alert the population.

Originally, InaTEWS aimed to detect tsunamis based on seismic parameters. However, unforeseen issues arose when the tsunamigenic source was not triggered by tectonic activity, leading to what is referred to as an atypical tsunami. The first

Submitted: 02-Oct-2023
Approved: 18-May-2024

Associate Editor: Eduardo Siegle

two observed atypical tsunami events occurred respectively in Palu Central Sulawesi Province in September 2018 and in the Krakatoa Mount in Sunda Strait in December 2018 (Triyono et al., 2019; Kongko et al., 2020; Nakata et al., 2020; Dogan et al.,2021; Fatimah et al., 2022). The most recent atypical tsunami was due to eruption of seamount volcanic Tonga on January 14th 2022.

Indonesia also faces short-distance tsunamis, in which the seismic vibration of the seafloor interferes with the detection of tsunami waves. This event vibrates the sensor on the seafloor, resulting in incorrect measurements of the hydrostatic pressure used to detect tsunami waves. The effort to remove the seismic signal data on the Bengkulu tsunami event in July 2007 (Pandoe et al., 2008) was unsuccessful because the seismic and tsunami frequencies interfered within data from the 15-second sampling period tsunami buoy system.

It is well-researched that tsunami waves in the deep sea last for a few minutes to several hours (Wiegel, 2005). Tsunami waves ride the tidal wave, but for a period far below tidal wave components. On the other hand, the seabed vibration due to seismic EQs has a very short period (Ouchi, 1981; Kobayashi et al., 2015). Thus, the length of tsunami waves lies between the period of the seismic signal and the tidal wave. So, it can be theoretically isolated by filtering the data from wave signal sampling appropriately.

Also, to overcome the vandalism problem on the buoy-based tsunami detection system, the Indonesian National Research and Innovation Agency (BRIN, previously the Indonesian Agency for Assessment and Application of Technology - BPPT) has developed a new system called Cable-based Tsunameter, in which Ocean Bottom Units (OBU) that contains specified sensors sitting on the seabed are connected to an on-shore station by a submarine repeatered optical cable commonly used in telecommunication. The structure of such submarine cable is shown in Figure 1. The center of the cable has a stainless-steel tube with 12 fiber-optic cores inside. The tube is protected by a galvanized steel wire armor. A thin tube of copper stretches along the outside of the wire armor. The copper tube acts as one electrical pole and the return pole consists of seawater. The copper is overlayed by a high density polyethylene dielectric. The dielectric is covered by a water repellent sheath and is protected by another galvanized steel wire. The outermost layer of cable is a polypropylene with bitumen that acts as an outer serving.

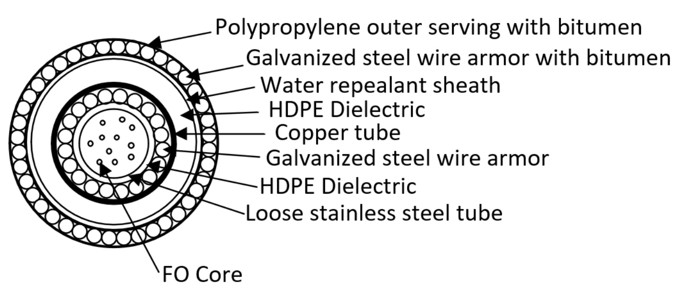

Figure 1. Internal structure of submarine cable.

Recently, a prototype system has been completely configured for operational testing in the Flores Sea, offshore to the north of Labuan Bajo in the East Nusa Tenggara Archipelago Province, Indonesia. This prototype is a single-ended system whose cable end sits at depth of 4,121 m. Moreover, two OBUs, the primary OBU LBB-02, have been installed at position 7° 59.7063 S 119° 56.1812 E at a depth of 4,121 m, 54 km away from the coast and the backup OBU LBB-01 closer to the coast at 8°10.5014 S 119° 55.2875 E at 2,110m deep, 34 km away from the coast. Each OBU contains a Paroscientific hydrostatic bottom pressure sensor 8CB700-I and Analog Device three-axis accelerometers ADXL-355 that can detect and measure water column pressure, sea water temperature, and sea floor vibration and other sensors to measure temperature, humidity, and leakage inside the OBU (Privadi et al., 2021). In total, these two OBU sets consistently measure the hydrostatic pressure with a sampling rate of 1 Hz and three-axis acceleration with a high sampling rate of 125 Hz. BRIN was installed in early March of 2022 and has been working since then (Kusuma et al., 2022; Purwoadi et al., 2023).

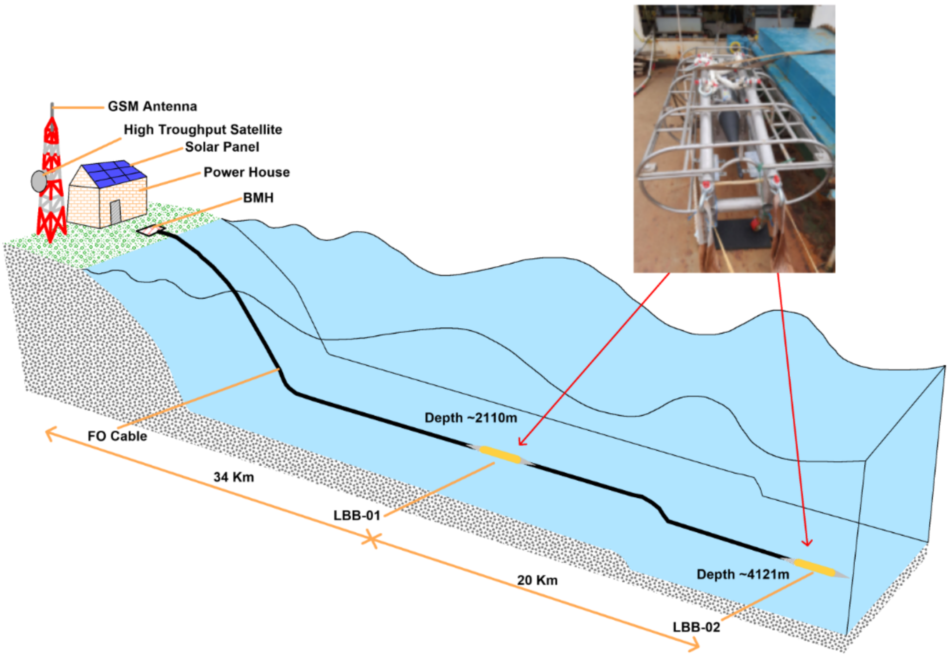

Figure 2. The configuration of InaCBT Labuan Bajo, with a 54-km fiber-optic cable. The OBU LBB-01 is located 34 km offshore at a depth of 2110m, whereas LBB-02 lies 54km offshore at a depth of 4121m. The Ocean Bottom Unit (OBU) has a stainless-steel frame.

As shown in Figure 2, the OBU is powered, internet-connected, and remotely operated from a landing shore station. So far, continuous data transmission of the real-time measurements has been properly performed during recent operational tests since early March 2022, with a data return above 96%. However, this study will only evaluate data from the primary pressure sensor LBB-02.

The ultimate objective requirement of the system is a fast and accurate detection of tsunami waves by identifying tsunami signals among wave spectrum measured by hydrostatic sensors containing noise and seismic and tsunami waves (Shinohara et al., 2015). This study reports the existence of long-period waves since the beginning of the signals measured by the hydrostatic sensor on primary OBU LBB-02 in case of a tsunami event caused by the M7.5 Banda Sea EQ on January 9th, 2023.

INACBT METHODS

To separate tsunami signals from others, the data filtering method applies the Lanczos filtering formula. This Fourier method reduces the energy of raw data at a specific frequency (given as cut-off period - CoP) (Duchon, 1979). Lanczos filtering is commonly used as a low-pass filter for time series data that can separate high- and low-pass frequencies at a selected cutoff period. (Aguilera, 2022; Lanczos Resampling, 2023; Low-Pass Filter, 2023). It functions as a low-pass filter, resulting in a number of data points (*numpt*) from *numpt+1+numpt* data input in a selected cut-off frequency (Figure 3), with a sampling rate in cycles per data interval (cpdi). *Numpt,* called the Kernel length, is identical to the number of data needed before and after the evaluated raw data points (the data at the time in which the event occurs). InaCBT uses a sampling rate of 1 Hz or 1-second sampling period.

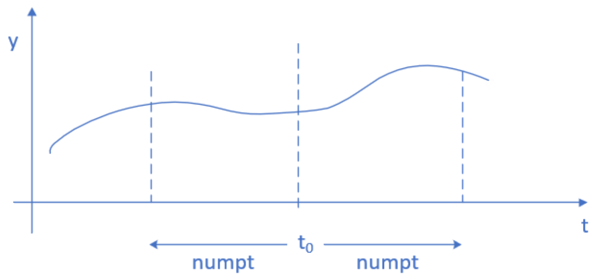

Figure 3. The Lanczos filter needs *numpt* data points before and after the point time of interest.

Figure 4 shows how the *numpt* length leads to the sharpness and accuracy of the applied Lanczos filter to the normalized data. The larger the *numpt,* the sharper the Lanczos filter function. A *numpt*=120 (i.e., 120 seconds) shows a gentle slope transition at the cutoff period of 40 seconds, whereas a *numpt*=300 (or 300 seconds) sharply decreases the relative power from 1 at T=43 sec to at T=35 sec. Furthermore, a *numpt* = 300 applies to the Kernel length of the Lanczos filtering in this study. It consequently leads to signal analysis being performed at least five minutes after the main earthquake and/or tsunami events to better filter results at the selected cutoff period.

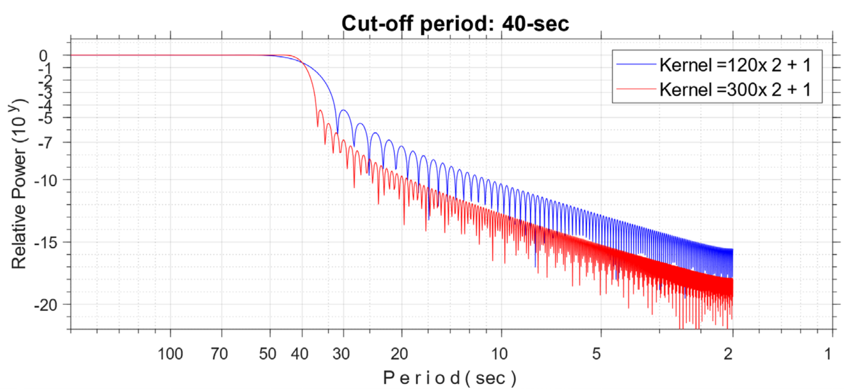

Figure 4. The Lanczos low-pass filtering function has a cut-off period of 40 seconds. The response Lanczos filtering curves were simulated with Kernel lengths equal to 120 (blue) and 300 (red).

Generally, the raw data spectrum has considerably higher energy than the filtered one, especially at shorter periods than the CoP, suggesting that the energy from high frequency has been suppressed. The operator determines the cut-off frequency at the receiving station upon evaluating the spectra energy of the raw data. This process expects that seismic, tsunami (seismic and atypical), and noise data can be correctly identified on the output display (Mizutani et al., 2020).

Although tsunami waves in the deep sea have its period from several minutes to several hours, Lacanna and Ripepe (2020) estimated that near-field and atypical tsunami wave periods vary from 50 to 120 seconds. Therefore, to avoid missing information for the possible occurrence of near-field and atypical tsunamis, we can choose the cut-off period within 30-50 seconds.

DATA ANALYSIS AND RESULTS

Since its deployment in early March 2022, the InaCBT has detected, among other things, three EQs and one tsunami, which occurred on January 9, 2023 due to the Banda Sea M7.9 earthquake. This study will discuss the following events: two distant EQs and a near-field EQ. See Table 1 and Figure 5. The corresponding detected EQs in Figure 5b refer to these that occurred in Flores, Bengkulu, and the Banda Sea.

Those distant earthquakes are mostly deep EQ hypocenters with a magnitude greater than M6.5

and a distance epicenter to the sensor LBB-02 of more than 2000 km. If a tsunami occurs, we will consult the tidal gauge to verify its impact on shore. Those detections will be compared with our new filtering method below.

Each of the three EQs that triggered the InaCBT are evaluated similarly. Measuring ocean wave power spectral density (PSD) aims to describe the dominant waves in the signal as a function of frequency per unit frequency. The Fast Fourier Transform (FFT) is calculated from the raw and filtered data. The raw data at LBB-02 undergoes treatment by a Lanczos low pass filter. The resulting series was obtained at a one-second data interval that will be compared to the raw data.

Overall, three data analysis cases are explained individually to illustrate their differences and similarities. Figures 6 to 8 show the power spectra from raw data for each EQ event component.

Table 1. Three detected earthquakes up to March 2023 by the InaCBT Labuan Bajo LBB-02.

Epicenter Location	Date	Time (UTC)	Lat	Depth km	Dist. (km)	Arrival Time (UTC)	Travel Time (minute)	Prop. Velocity* (km s^{-1})
			Long	Mag				
Flores	23 Jul 2022	06:09	7.65° S 122.43° E	11 5.4	277	06:10	1	4.6
Bengkulu	18 Nov 2022	13:37	4.880° S 100.65° E	10 6.8	2165	13:51	14	2.57
Banda Sea	9 Jan 2023	17:47	7.37° S 130.23° E	136 7.5	1136	17:50	3	6,31

*Note: EQ wave type propagation: Primary - 5 – 6 km s^{-1}

Secondary - 3 – 4 km s^{-1}

Tertiary - < 3 km s^{-1}

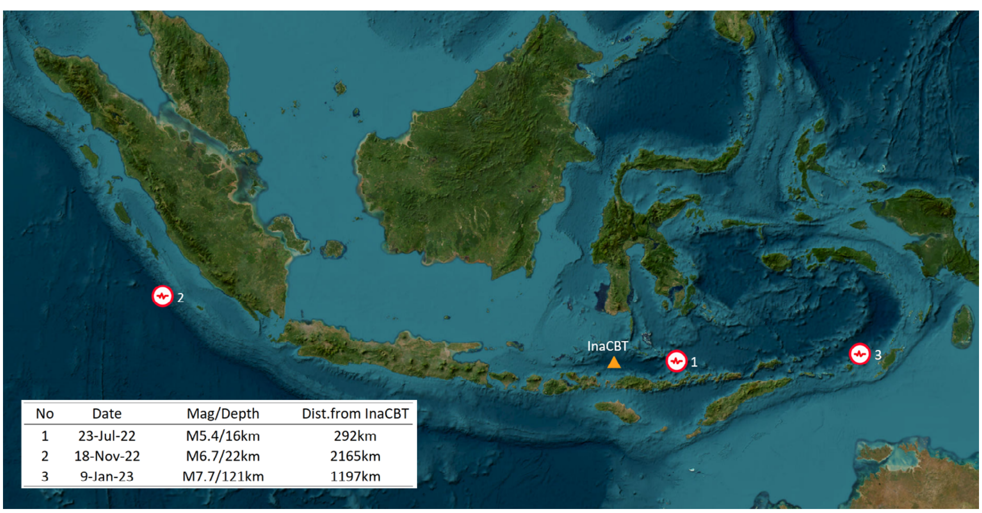

(a)

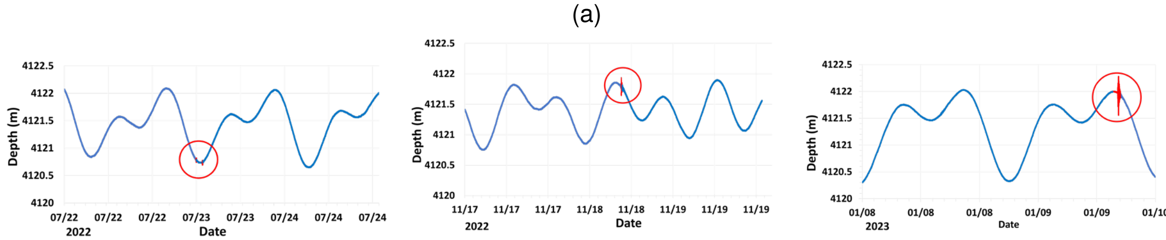

(b)

Figure 5. (a) InaCBT LBB-02 recorded three EQ epicenters. **(b)** The red circles mark the time in which the EQs occurred: Flores, July 23, 2022 (left); Bengkulu, November 18, 2022 (center); Banda Sea, January 9, 2023 (right); Time refers to UTC.

Earthquake Flores – July 23, 2022, 06.09 UTC

The first case refers to the EQs the epicenter of which occurred twice in the Flores Sea, on July 23, 2022, at 06.09 and 07.35 UTC, respectively (Figure 6). These near-field EQs occurred only about 280 km from the LBB-02 and were detected twice at 6:10 and 7:35, respectively, with only one minute of wave travel time from the EQ sources to the LBB. Since the distance between the epicenter and LBB is relatively small, estimating the propagation velocity is improper.

The raw data time series underwent Lanczos low-pass filtering with a cut-off period of 40 seconds. Spectral analysis compared the spectral density between the raw and filtered data (Figure 6, bottom). The spectral density plot shows that the raw data has slightly stronger signals from 10 to 15 seconds, such as swell-like seismic wave signals.

The spectral density of low-pass filtered data shows that the power spectral is suppressed at the cut-off period to separate seismic, tsunami, and other longer-period signals. The plot of low- and high-pass filtered data (Figure 6, middle) separates the tide from the seismic tremors. Theoretically, in case of a tsunami, the signals must appear in this low-passed curve. The high frequency (i.e., short-period) signals with a period less or equal to 40 sec appear in this high pass filtered data, including the seismic signals originating from both the Flores EQ and background noises (Figure 6, bottom).

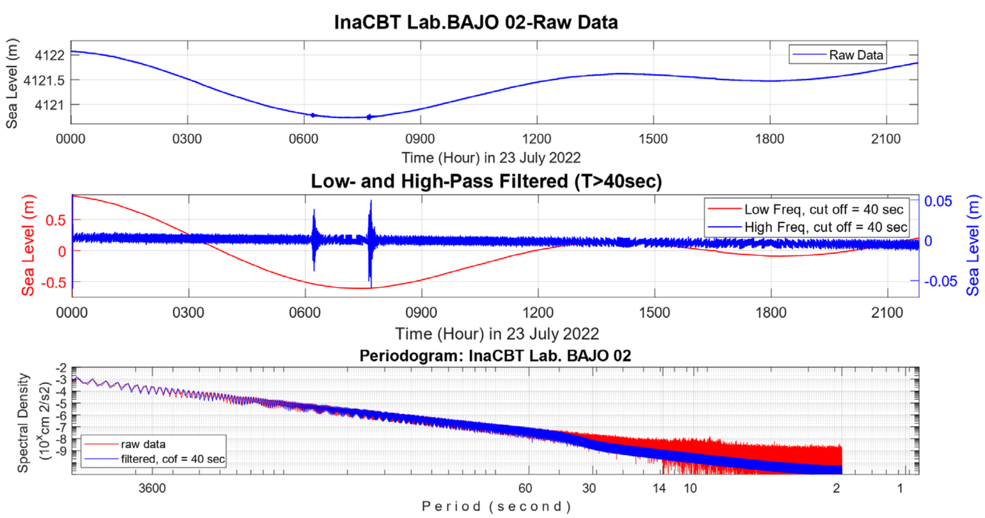

Figure 6. Two Flores EQ events on July 23, 2022 at 06:09 UTC and 07:35 UTC. (**Top**) Raw time series the x-axis of which represents time in UTC (hhmm) and the y-axis, pressure depth in meters. (**Middle**) A 40-second CoP filters the original time series with two spikes. The resulting time series shows the low- (red) and high-pass (blue) filtered time series (blue). (**Bottom**) The spectra for raw data (red) show weak signals for the recorded wave at the 10-14 sec wave period, and the filtered spectra (blue) suppressed high frequency/short period signals.

EQ Bengkulu, Nov 18, 2022, 13:37 UTC

The second case refers to the EQ on November 18, 2022, at 13:37 UTC, with a 6.8-magnitude epicenter in the western Indian Ocean offshore Bengkulu, Sumatra. The hypocenter depth lies at 10 km but no tsunami occurred. The distance from the LBB totals about 2,165 km, and it was detected at the LBB at 13:51, or 14 minutes after the initial shock. The wave propagation totals about 2.57 km s^{-1}, lying within the range of tertiary waves (Figure 7 - top)

A low-pass Lanczos filtering technique was applied to the raw data time series, with a 40-second cut-off period. Spectral analysis compares the spectral density between the raw (Figure 7, - bottom - red) and filtered data (Figure 7, - bottom - blue). Spectral density shows that the raw data has significant strong signals from 10 to 14 seconds, peaking at 12 seconds.

Ocean wave spectra classify the “swell” wave period that can be identified within 10-20 seconds (Wiegel, 2005). The Pressure Response Factor given by Dean and Dalrymple (1984) suggests that shorter waves (higher frequency) will diminish as the pressure sensor goes deeper. Surprisingly, the periodogram as a response to a seismic wave due to an earthquake shows a strong high-frequency signal at 10-14 seconds in depths below 2000 m, as shown in the spectral density plot. It is nearly similar to the period of a swell wave. When no EQ tremors exist in the raw data, these signals fail to appear. It is then called a swell-like seismic wave signal.

The spectral density of low-pass filtered data shows that the power spectral is suppressed at the cut-off period of 30 seconds to separate seismic and tsunami (if present) signals from other data for a longer period. The low-pass filtered data (Figure 7 – middle - red) is free from seismic signals and noises. The signals must arise in this low-passed time series window if a tsunami wave is present. The high frequency (i.e., short period) signals with a period less or equal to 30 sec appear in this high pass filtered time series, including the seismic signals originating from the Bengkulu EQ and noises (Figure 7, - middle - blue). It is interesting to explore the existence of swell-like seismic waves with a maximum wave height H=0.3 m but such research lies beyond the scope of this study.

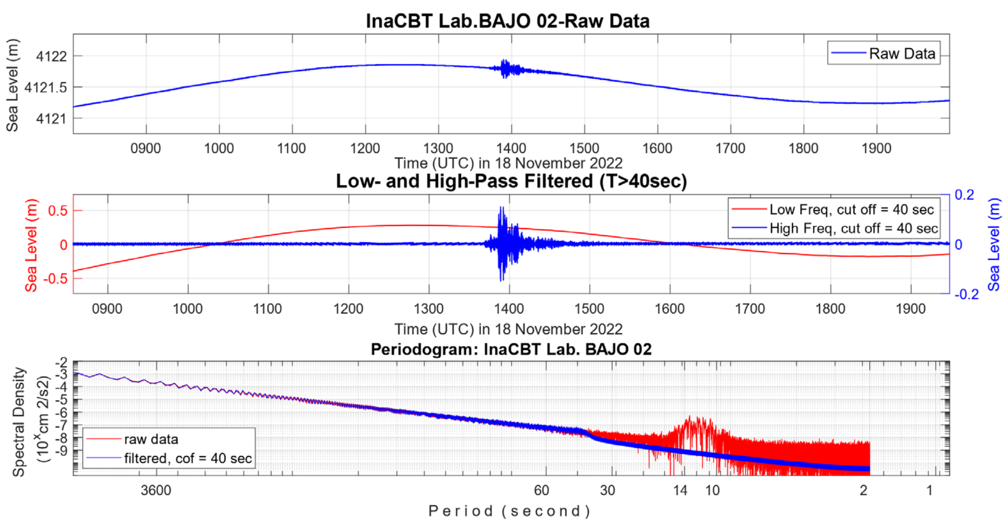

Figure 7. The Bengkulu EQ on November 18, 2022 at 13:37 UTC: signals recorded in LBB-2. (**Top**) Raw time series data the x-axis of which represents time (hhmm) and the y-axis, pressure depth in meters. (**Middle**) Strong spikes are filtered by a 40-second CoP, resulting in the identification of low-pass and high-frequency time series data, respectively. (**Bottom**) The spectra for raw data (red line) show strong signals for the recorded wave at the 10-14 sec wave period, and the filtered spectra (blue line) reduced high-frequency data.

EQ Banda Sea, Jan 9, 2023, 17:47 UTC

The third case refers to the Banda Sea EQ on January 9, at 17:47 UTC, with a M7.5-magnitude epicenter in the Banda Sea. Its hypocenter lied at a 131 km depth. Its distance from the LBB totals about 1,131 km, and it was detected at 17:50 (three minutes after the initial shock). The wave propagation totals about 6.5 km s^{-1}, lying within the range of primary waves. The cut-off of the Lanczos filter is set to 40 seconds. Unlike the previous events, its low-frequency signals were not flat. It contained some fluctuation (red colored in Figure 8) that shows the existence of certain period waves, such as tsunami or other waves that arrive sooner than the main wave. In total, six National Geospatial Information tidal gauges, placed at several islands in the Banda Sea, detected the rise of the sea surface by 5-9 cm 20-32 minutes after the EQ, confirming the tsunami wave (National Centers for Environmental Information, 2023).

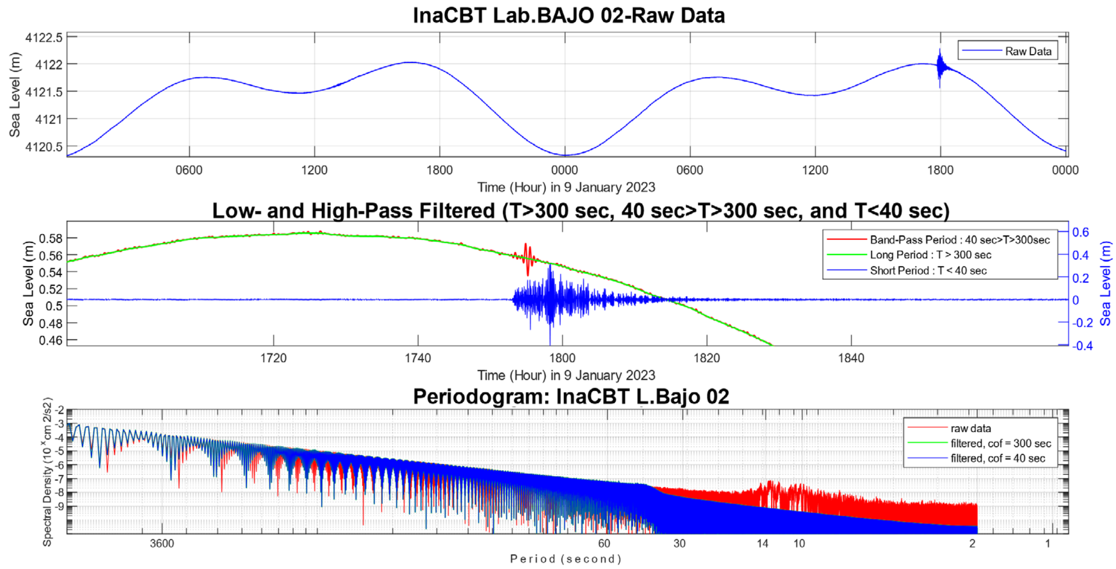

Figure 8. The Banda Sea EQ on January 9, 2022 at 17:47 UTC: signals recorded in LBB-2. (**Top**) Raw time series data the x-axis of which represents time (hhmm) and the y-axis, pressure depth in meters. (**Middle**) Strong spikes are filtered by a 40- and 300-second CoP, identifying low-pass, 40-300-second band pass, and high-pass filtered time series, respectively. (**Bottom**) The spectra for raw data (red) show weak signals for the recorded wave at the 10-14 sec wave period, and the filtered spectra (blue) suppressed high frequencies.

DISCUSSION

Wave periods from 10 to 15 seconds show prominent energy peaks in all studied earthquake events, which are associated with seismic signals due to events in near- and far-field earthquakes. This shows why the data from the tsunami buoy could not be used since its sampling period is 15 seconds, which is too close to the range of the interesting period. So, the cut-off of the Lanczos filter was set at 40 seconds to conserve the higher period wave.

In the case of the Banda Sea event, the filtered signal contained a low-frequency signal whose periods exceeded 40 seconds. The signal directly results from applying the Lanczos filter to the raw signal. However, it is a body wave since it came a few minutes early before the maximum recorded signal of the earthquake. If it were a tsunami wave — whose propagation speed totals around 800 km/hour —, the signal should be detected more than one hour after the earthquake. It also fails to constitute an acoustic wave since its speed only totals around 1.5 km s^{-1}. With a speed of around 6.5 km s^{-1}, the signal could be a seismic primary wave propagating on the crust of the earth. This significant finding shows that primary seismic waves contain a low-frequency signal with a period that exceeds 40 seconds. According to (Ouchi, 1981), the period of P-wave lies at 0.1-0.17 seconds for an event with S-P times greater than 50 seconds, and according to (Kobayashi et al., 2015), the P-wave period lies at 1.3-0.08 second, which is very far from a 40-second CoP.

Evaluating the bandpass period clearly shows that the individual wave envelope with a period from 40 to 300 seconds has been detected as the initial wave (Figure 8, red line). Learning from the properties of body and surface seismic waves, this band-passed wave (40<T<300) is classified as body waves (P- and/or S-waves). Body waves travel mainly in the ground or shore layers and are faster than surface waves. Body waves arrive from two to three minutes earlier than the following surface waves (Figure 8, blue line), but they are not tsunami waves. Another inspection was performed to determine the limit of the existing body wave period under a 300-second CoP (Figure 8, green line). In this inspection, body waves decrease at T = 300 sec or longer. The maximum amplitude of the earthquake shaking wave emerges 2-3 minutes after the initial tremors generated by the ground shaking.

It is interesting to explore how this low-frequency signal can be "modulated" in the high-frequency P-wave signal.

This system offers a novelty in data processing to quickly evaluate during EQ and potential tsunami events. The operator at the data center can dispense with removing tidal components analysis and detiding as a standard procedure implemented in tsunami buoys. This new approach can quickly and directly confirm tsunamis by low-pass filtering to separate one and other dominant signals.

CONCLUSION

Indonesia has successfully designed, manufactured, and launched the prototype of an Indonesian Cable-based Tsunameter in the Flores Sea, lying offshore to the north of Labuan Bajo on the west coast of Flores Island of Indonesia since March 2022. It works well and continuously transmits data with 1 Hz sampling from two OBUs to detect the tsunami. The CBT detected several distant and near-field earthquakes, which generated a swell-like seismic wave with a period from 10 to 15 seconds.

In the case of the Banda Sea EQ, the primary seismic wave contained a low-frequency long-period signal that could be extracted using the Lanczos filter with a specified number of Kernel lengths and a cut-off period from 30 to 50 seconds. If we can prove that this long-period signal is the "precursor" of a tsunami wave, this new approach should speed up operators' or authorities' decision making. The system detects sea level anomalies by a more direct evaluation regarding both its time- and frequency-domain, without analyzing tidal harmonic analysis.

On the other hand, there remains the question of how distant earthquake signals propagate through the water column or ground layers until LBB-02 detects it and why the swell-like seismic signals have wave heights of up to 0.3 m and peak periods from 10 to 15 seconds. The sampling rate of 1 Hz may need to be improved to 25 Hz or higher. Using a similar procedure to the in one this study, wave peaks could be shifted or still show similar results. Another prototyping might be considered, whereas the recent prototyping can be applied in test operations or be made ready for market delivery. These up- and downstream developments promise to improve near-field and atypical tsunami detection.

ACKNOWLEDGMENTS

Funding for this study was provided by the National Research and Innovation Agency (BRIN) of the Republic of Indonesia under the national program the Indonesian Tsunami Early Warning System (InaTEWS), FY 2021, and the Technology for Disaster (Tekcana), FY 2022.

AUTHOR CONTRIBUTIONS

W.W.P.: Investigation, Conceptualization, Visualization, Resources, Methodology, Software Project administration, Validation, Writing – Original Draft.

M.A.P.: Conceptualization, Investigation, Formal analysis, Writing - Review & Editing.

Z.Q.: Software Validation, Formal analysis, Visualization, Writing - Review & Editing.

A.R.: Data curation, Software Validation, Visualization, Writing - Review & Editing.

A.S.: Resources, Data curation.

REFERENCES

Aguilera, C. A. V. 2022. *LanczosFilter.m*. MATLAB Central File Exchange. Available from: https://www.mathworks.com/matlabcentral/fileexchange/14041-lanczosfilter-m Access date: Jul 28, 2022.

Dean, R. G. & Dalrymple, R. A. 1984. Water wave mechanics for engineers and scientists. *Eos*, 66(24), 490-491. DOI: https://doi.org/10.1029/eo066i024p00490-06

Dogan, G. G., Annunziato, A., Hidayat, R., Husrin, S., Prasetya, G., Kongko, W., Zaytsev, A., Pelinovsky, E., Imamura, F. & Yalciner, A. C. 2021. Numerical Simulations of December 22, 2018 Anak Krakatau Tsunami and Examination of Possible Submarine Landslide Scenarios. *Pure and Applied Geophysics*, 178(1), 1–20. DOI: https://doi.org/10.1007/s00024-020-02641-7

Duchon, C. E. 1979. Lanczos Filtering in One and Two Dimensions. *Journal of Applied Meteorology*, 18, 1016–1022.

Fatimah, S., Hafidz, A., Zikri, M. S., Safira, N., Indra, T. L. & Supriyanto. 2022. Landslide triggered tsunami modelling: A study in Anak Krakatoa collapse. *E3S Web of Conferences*, 340, 1–5. https://doi.org/10.1051/e3sconf/202234001003

Kobayashi, M., Takemura, S. & Yoshimoto, K. 2015. Frequency and distance changes in the apparent P-wave radiation pattern: Effects of seismic wave scattering in the crust inferred from dense seismic observations and numerical simulations. *Geophysical Journal International*, 202(3), 1895–1907. https://doi.org/10.1093/gji/ggv263

Kongko, W., Karima, S. & Daryono. 2020. The Tsunami Model of Mount Anak Krakatau Landslide in 2018 and Its Future Potential Hazard to the Coastal Infrastructures in Sunda Strait. *Journal of Physics: Conference Series*, 1625(1). DOI: https://doi.org/10.1088/1742-6596/1625/1/012052

Kusuma, A. A. N. A., Agastani, T., Nugroho, T., Anggraeni, S. P. & Hartawan, A. R. 2022. Estimating MQTT Performance in A Virtual Testbed of INA-CBT Communication Sub-System. *In*: *Proceeding - 2022 International Conference on Radar, Antenna, Microwave, Electronics, and Telecommunications: Emerging Science and Industrial Innovation in Electronics and Telecommunication*, ICRAMET 2022 (pp. 73-77). DOI: https://doi.org/10.1109/ICRAMET56917.2022.9991213

Lacanna, G. & Ripepe, M. 2020. Genesis of Tsunami Waves Generated by Pyroclastic Flows and the Early-Warning System. *Miscellanea INGV*, 255.

Lanczos resampling. 2023. Wikipedia. Available from: https://en.wikipedia.org/wiki/Lanczos_resampling Access date: Jan 12, 2023

Low-pass Filter. (2023). Wikipedia. Available from: https://en.wikipedia.org/wiki/Low-pass_filter. Access date: Jan 12, 2023

Mizutani, A., Yomogida, K. & Tanioka, Y. 2020. Early Tsunami Detection With Near-Fault Ocean-Bottom Pressure Gauge Records Based on the Comparison With Seismic Data. *Journal of Geophysical Research: Oceans*, 125(9). DOI: https://doi.org/10.1029/2020JC016275

Nakata, K., Katsumata, A. & Muhari, A. 2020. Submarine landslide source models consistent with multiple tsunami records of the 2018 Palu tsunami, Sulawesi, Indonesia. *Earth, Planets and Space*, 72(1). https://doi.org/10.1186/s40623-020-01169-3

National Centers for Environmental Information. 2023. *Tsunami Event Banda Sea*. Silver Spring: NCEI. Available from: https://www.ngdc.noaa.gov/hazel/view/hazards/tsunami/runup-more-info/36972 Access date: Feb 17, 2023

Ouchi, T. 1981. Spectral Structure of High Frequency P and S Phases Observed by Obs's in the Mariana Basin. *Journal of Physics of the Earth*, 29, 305–326.

Pandoe, W. W., Djamaluddin, R. & Kongko, W. 2008. The 12 September 2007 Tsunami Detected on Indonesian "Krakatau" Tsunameter. *In*: *International Conference of the Tsunami Warning, Ministry of Research and Technology of the Republic of Indonesia*, Bali.

Privadi, A., Damara, D. R., Widati, P. L. & Triputra, F. R. 2021. Indonesia's Cable Based Tsunameter (CBT) System as an Earthquake Disaster Mitigation System in East Nusa Tenggara. *Proceeding - 2021 IEEE Ocean Engineering Technology and Innovation Conference: Ocean Observation, Technology and Innovation in Support of Ocean Decade of Science*, OETIC 2021 (pp. 63-67), Jakarta. DOI: https://doi.org/10.1109/OETIC53770.2021.9733734

Purwoadi, M. A., Anantasena, Y., Pandoe, W. W., Widodo, J. & Sakya, A. E. 2023. Introduction to Indonesian Cable-based Subsea Tsunameter. *2023 IEEE International Symposium on Underwater Technology*, UT 2023, March (pp. 1-6), Tokyo. DOI: https://doi.org/10.1109/UT49729.2023.10103368

Shinohara, M., Yamada, T., Sakai, S., Shiobara, H. & Kanazawa, T. 2015. New ocean bottom cabled seismic and tsunami observation system enhanced by ICT. *2014 Oceans - St. John's, OCEANS 2014*, St. John's. DOI: https://doi.org/10.1109/OCEANS.2014.7003045

Triyono, R., Prasetya, T., Anugrah, S. D., Sudrajat, A., Setiyono, U., Gunawan, I., Priyobudi, Yatimantoro, T., Hidayanti, Anggraini, S., Rahayu, R. H., Yogaswara, D. S., Hawati, P., Apriyani, M., Julius, A. M., Harvan, M., Simangunsong, G. & Kriswinarso, T. 2019. Katalog Tsunami Indonesia Per-Wilayah Tahun 416-2018. *In*: *Pusat Gempabumi dan Tsunami Kedeputian Bidang Geofisika*. Jakarta: BMKG.

Wiegel, L. R. 2005. Oceanographical Engineering. In: Wiegel, L. R. *Prentice-Hall international series in theoretical and applied mechanics Prentice-Hall series in fluid mechanics* (pp. 532). [S. l.]: Prentice-Hall.